Available online at www.sciencedirect.com
SCIENCE DIRECT®
Journal of Molecular Catalysis A: Chemical 238 (2005) 63–71
JOURNAL OF MOLECULAR CATALYSIS A: CHEMICAL
www.elsevier.com/locate/molcata

TiO_2: As a versatile catalyst for the ortho-selective methylation of phenol

Aditi R. Gandhe [a], Julio B. Fernandes [a,*], Salil Varma [b], N.M. Gupta [b]

[a] *Department of Chemistry, Goa University, Talegao Plateau, Goa 403206, India*
[b] *Catalysis Division, BARC, Mumbai 400085, India*

Received 22 March 2005; received in revised form 3 May 2005; accepted 5 May 2005
Available online 13 June 2005

Abstract

The investigation describes synthesis of active pure and mixed phase TiO_2 catalysts by a $TiCl_3$–urea–oxalic acid precursor method. Pure and mixed phase TiO_2 catalysts could be obtained by varying the concentration of oxalic acid during synthesis. A minimum of 25 mol% of oxalic acid during synthesis was found to bring about complete phase transition from rutile to anatase. The catalysts were characterized by XRD, BET surface area measurements, pore-size analysis, TPD studies with NH_3 and CO_2 as probe molecules for acidity and basicity. In situ FTIR studies using pyridine as a probe molecule for determining the type of acid sites. The various TiO_2 catalysts were evaluated for the methylation of phenol reaction. While all the samples were near100% ortho-selective, they showed a unique activity profile as the concentration of oxalic acid was increased during the synthesis. The observed yield and product selectivity is correlated with the surface properties of the catalysts. The overall catalytic activity did not show particular phase dependence. Strong Lewis acid–weak Lewis base pairs were identified as the active centers for ortho-selectivity. The catalytic activity was primarily governed by the concentration of effective strong Lewis acid–weak Lewis base pairs. The selectivity between the ortho-products *o*-cresol and 2,6-xylenol is greatly influenced by the pore-size distribution.

Keywords: Phenol; Ortho-selective methylation; TiO_2

1. Introduction

Alkylation is an industrially important organic reaction. Alkyl phenols are important chemicals and chemical intermediates in the agrochemical and pharmaceutical industries. While the *o*-alkylated product anisole is used in the synthesis of anethole in the beverage industry, the ortho-products *o*-cresol and 2,6-xylenol are particularly important. They are used as intermediates in the synthesis of PPO resins. Since methylation of phenol is an important reaction a large number of catalyst systems like oxides, mixed metal oxides, ferrospinels as well as zeolites have been investigated so far. While most present day catalyst form a mixture of products, others show instability with time on stream due to coking. Hence search for appropriate catalyst system continues [1].

The optimum reaction temperature and product selectivity are primarily governed by the type of active centers on the surface of the catalyst. Depending on the type of active centers, viz. Lewis or Bronsted, the orientation of the phenol molecule varies and so does the product selectivity. While catalysts with Lewis acid sites are known to be ortho-selective, those with Bronsted acid sites form a mixture of products.

We have recently investigated methylation of phenol [2,3] on commercial and synthetic TiO_2 catalysts. Both rutile and anatase catalysts have been tested. A rutile TiO_2 synthesized using $TiCl_3$–urea precursor was found to be 100% ortho-selective at an optimum conversion of 42% at 450 °C [2]. The ortho-selectivity was attributed to the presence of weak basic sites, as evident from the low temperature peak ~150 °C in the TPD CO_2 spectra. The unique weak basic sites were

* Corresponding author. Tel.: +91 832 2518145; fax: +91 832 2452889.
E-mail address: juliofernandes@rediffmail.com (J.B. Fernandes).

1381-1169/$ – see front matter © 2005 Elsevier B.V. All rights reserved.
doi:10.1016/j.molcata.2005.05.011

believed to have its origin in the urea related synthesis strategy employed.

Use of carboxylic acid during the synthesis of TiO_2 samples has been reported to have a favourable effect on their surface properties, resulting in mesoporous titania with high surface areas [4]. We report here the synthesis of TiO_2 using urea–oxalic acid precursors. The resulting TiO_2 was highly active for the methylation of phenol while retaining its high ortho-selectivity.

2. Experimental

2.1. Catalyst synthesis

Synthesis of the rutile TiO_2 (R2) using $TiCl_3$ and urea in the molar ratio of 1:2 is described earlier [2]. Synthesis of catalysts using oxalic acid was carried out essentially by the same procedure as R2. Thus, calculated quantity of $TiCl_3$ was taken in an evaporating dish, followed by the drop-wise addition of 0.5 M HNO_3, till the colour changed from violet to colourless. This was followed by addition of urea and oxalic acid such that the $TiCl_3$:oxalic acid:urea molar ratio in the final mixture was 1:1:2. The resulting mixture was then evaporated to dryness on a steam bath. The dry residue was transferred to a glass column and heated in a horizontal muffle furnace at 400 °C, with continuous flow of dry air for 5 h. The resultant solid was then cooled to ambient temperature and then homogenized to obtain the final samples. Four additional TiO_2 samples were prepared by varying the oxalic acid content between 0 (as for R2) and 1 mol (as for A2), in steps of 0.2 mol of oxalic acid (Table 1).

2.2. Catalyst characterization

2.2.1. XRD

The X-ray powder diffraction patterns (XRD) have been recorded on a Shimadzu LabX −700 diffractometer, using Ni filtered Cu Kα radiation (λ = 1.5406 Å) by step scanning with a scan rate of 2° 2θ/min (Fig. 1). The crystallite size was determined by Scherrer formula. The weight percent of anatase in the rutile phase was obtained from the equation [5].

$$X_A = \left[1 + 1.26\left(\frac{I_R}{I_A}\right)\right]^{-}$$

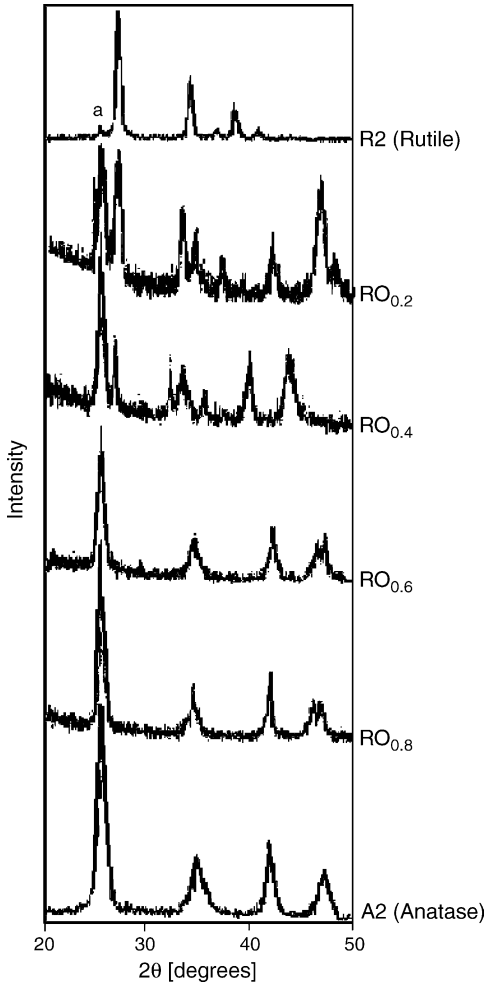

Fig. 1. XRD profiles of pure and mixed TiO_2 phases A2, pure anatase; R2, pure rutile.

where X_A is the weight fraction of anatase in the mixture, I_R and I_A are obtained from the peak areas of the characteristic anatase (1 0 1) and rutile (1 1 0) diffractions, respectively.

2.2.2. BET surface area

Nitrogen adsorption and desorption isotherms were collected at −196 °C on a Quantachrome Autosorb 1 sorption analyzer. All the samples were outgassed for 3 h at 250 °C under vacuum in the degas port of the adsorption analyzer. The specific surface area was calculated using the BET model. The pore-size distributions were obtained from the desorption branch of the isotherm.

Table 1
Structural properties of the titania samples

Catalyst code	Oxalic acid (mol)	Phase	Percentage of anatase	Sherrer crystallite sizes (nm)	Surface area (m^2/g)
R2	0	Rutile	3.5	9.1	36
$RO_{0.2}$	0.2	Mixed	49.2	6.8	69
$RO_{0.4}$	0.4	Mixed	67.3	8.3	69
$RO_{0.6}$	0.6	Anatase	100	11.1	80
$RO_{0.8}$	0.8	Anatase	100	11.1	86
A2	1	Anatase	100	8.7	73

2.2.3. Temperature programmed desorption (TPD)

i. NH_3 is used as a probe molecule for the estimation of acidity.
ii. CO_2 is used as a probe molecule for the estimation of basicity.

TPD measurements were carried out in a muffle furnace. A known weight of the catalyst was packed in a glass column. Ceramic beads were used as pre-heaters. The catalyst was activated at 120 °C for about 2 h under flowing dry N_2. Before admitting the NH_3 vapours/CO_2 gas, the catalyst was allowed to cool to room temperature. Ammonia/carbon dioxide was passed over the catalyst for 45 min at a rate of 5 ml/h. The samples were then flushed with dry nitrogen at 110 °C, followed by heating at the rate of 5 °C/min to cause desorption. The desorbed gases, viz. NH_3 or CO_2 were bubbled in 0.03 M HCl or 0.04 M NaOH, respectively. Thus, the amount of gas desorbed was quantified by back titration. This amount desorbed at various temperatures is a measure of the catalyst acidity or basicity, respectively, and is expressed in micromoles per gram.

2.2.4. In situ FTIR

The type of acid sites, viz. Lewis or Bronsted were elucidated by in situ FTIR studies using pyridine as a probe molecule. The IR spectroscopic investigations of pyridine are very effective for studying the nature and amount of acid sites on metal oxides [6–9]. In situ FTIR studies were carried out in the temperature range of 25–350 °C. Prior to the experiment self-supported wafers of the samples, 2.5 cm in diameter were prepared by using about 80 mg of the sample. The wafer was then mounted in a high temperature, high-pressure IR cell fitted with water-cooled CaF_2 windows. A JEOL FTIR instrument equipped with a DTGS detector was used for the study. The wafer was mounted in the cell and at first evacuated at 120 °C for 24 h to make the surface clean, viz. free of adsorbed water and other gases. The wafer was then allowed to cool to room temperature. A blank spectrum was recorded. Subsequently they were exposed to pyridine vapours. The spectrum was recorded at room temperature. The temperature was then increased from ambient to 350 °C, in steps of 50 °C. Spectra were recorded at each temperature. The spectra for two of the samples R2 and A2 after 30 min evacuation at room temperature are as shown in the Fig. 3.

2.3. Methylation reactions

The methylation reactions were carried out in a vertical flow reactor. Prior to the reaction, 1 g of the catalyst sample was pelletized and crushed and then loaded in a glass reactor (i.d. = 30 mm). The catalyst was activated in flowing air for about 5 h at a temperature of 450 °C. The temperature was then brought down to the desired reaction temperature in dry nitrogen. Once the reaction temperature was attained the catalyst was allowed to remain at that temperature for 1 h prior to the reaction. In a typical reaction, a pre-optimized mixture of phenol:methanol in a molar ratio of 1:6 was fed into the reactor at pre-determined flow rates through a peristaltic pump (Miclins, India). The reaction was studied also at a pre-optimized flow rate of 5 ml/h and at temperatures between 250 and 480 °C. The products were condensed and analyzed by a Chemito 8610 GC using a FID detector and a SE 30 column.

3. Results and discussion

Fig. 1 gives the XRD patterns of the samples. The peaks marked '**a**' show the presence of the anatase phase. The sample R2 prepared by the calcination of acidified $TiCl_3$ in presence of urea showed a rutile crystal phase, with a trace amount of anatase phase as evident from a peak at $d = 3.50$ Å and $I/I_0 \sim 0.8\%$. On the other hand the sample A2 prepared with 1 mol of oxalic acid was a 100% anatase phase. As can be seen from Fig. 1 and Table 1, increasing addition of oxalic acid gave increasing percent of anatase phase. This was evident from the increased intensity of the characteristic anatase peak at $d = 3.50$ Å. When the concentration of oxalic acid was $\geq$0.6 mol, only anatase phase was observed.

The weight percent of anatase in the samples and Scherrer crystallite sizes are also reported in Table 1.

3.1. Reactivity of rutile (R2) and anatase catalyst (A2)

3.1.1. Activity and selectivity

Fig. 2 shows the comparative performance of the two catalysts for the methylation of phenol in the temperature range of 350–450 °C. Table 2 gives their relative catalytic activity in terms of percent conversion of phenol as well as selectivity. It is clear that A2 is more active than R2 under all temperatures investigated.

Thus, the rutile sample R2 prepared by the $TiCl_3$–urea method gave 40% conversion and 100% ortho-selectivity. On the other hand, A2, prepared with the additional use of oxalic acid was highly active. It was twice as active as R2, i.e. about 80% conversion and gave near 100% ortho-selectivity.

Further, it is interesting to note that, although the ortho-selectivity in both the catalysts, R2 and A2, were >98% there was a marked difference in the individual break up of the ortho-selectivity. While R2 was more selective towards *o*-cresol, A2 was more selective towards the more bulky 2,6-xylenol.

3.1.2. Type of active centers

The high ortho-selectivity in R2 as well as A2 during methylation of phenol is due to the existence of an acid–base pair mechanism. Such a mechanism has been reported earlier [10]. Thus, a phenol molecule interacts with a Lewis acid–base pair of the type Ti^{4+}–O^{2-}, dissociatively adsorbing as a phenolate ion on the acid site, while its proton interacts with the adjacent basic site. The proton thus generated activates methanol as a methyl carbocation, which then attacks

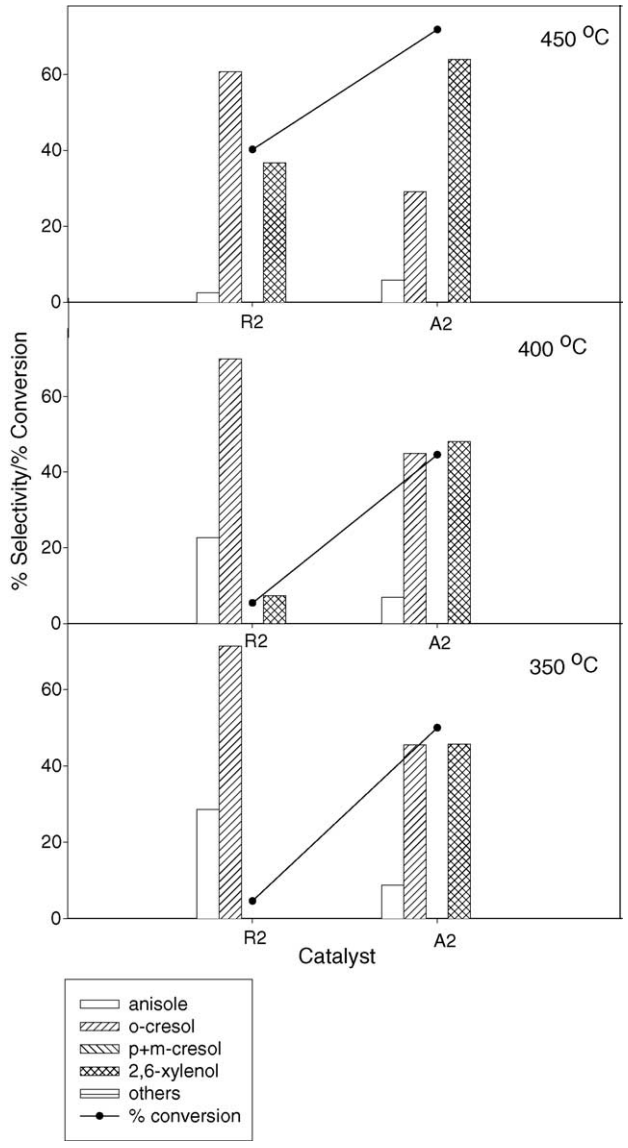

Fig. 2. Activity-selectivity profiles of R2 and A2, in the temperature range 350–450 °C, with 1 g of the catalyst, 1:6 phenol:methanol molar ratio and a flow rate of 5 ml/h.

the ortho positions of the ring, which are closer to the surface and thus results in high ortho-selectivity.

The presence of Lewis acidity is confirmed by in situ FTIR studies using pyridine as a probe molecule; see Fig. 3. These spectra are recorded as a function of evacuation temperature from ambient to 350 °C on catalyst R2. Table 3 gives the corresponding band assignments.

Table 3
IR absorption frequencies following adsorption of pyridine on catalyst R2

IR frequencies (cm^{-1})	Assignments
1114 w	Lw (weak Lewis acid sites)
1149 w	–
1217 w	Ls (strong Lewis acid sites)
1445 vs	Ls
1492 w	L + B combination peak
1540 vw	B (Bronsted acid sites)
1557 vw	B
1575 w	B
1605 vs	Ls

w, weak; vw, very weak; vs, very strong.

The intense bands at 1445 and 1605 cm^{-1} as well as the weak band at 1217 cm^{-1} are attributed to the presence of strong Lewis acid sites (Ls). These assignments are in agreement with those reported in literature for strong Lewis acid sites on rutile titania surfaces [11–13]. The weak bands at 1540, 1557 and 1575 cm^{-1} indicate presence of small amounts of Bronsted acid sites. Such bands are due to the presence of pyridinium ion PyH^+ [11,14]. The intensity of these peaks for the catalyst R2 is very weak even at ambient temperatures. This suggests that R2 is a predominant Lewis acid catalyst.

It is interesting to note that the intensity of Bronsted acid site band at 1575 cm^{-1} decreases with rise in temperature and almost vanishes at 350 °C. This is due to dehydroxylation of the bridged hydroxyl groups, causing additional Lewis acid sites. That Lewis acid sites can be generated through dehydroxylation of surface hydroxyls has been reported [15,16].

Further the band at 1492 cm^{-1} for R2 is the combination band [11,13,14] and has contributions from both Lewis as well as Bronsted acid sites. As seen from Fig. 3, as the temperature is raised, this band shows a reverse trend as that of the 1575 cm^{-1} band. Thus, as the 1575 cm^{-1} band intensity drops, there is a corresponding rise in intensity of the 1492 cm^{-1} band. These results confirm that as temperature is raised there is generation of Lewis acid sites. Thus, the band at 1492 cm^{-1}, could be largely due to Lewis acid sites.

It is also known that the relative intensities of the bands around 1450 and the 1570 cm^{-1} bands give the relative proportion of the type of Lewis and Bronsted acid sites, respectively [17]. As can be seen from Fig. 3, the relative intensities of the 1445 and 1575 cm^{-1} in R2 is >90%. Thus, R2 is predominantly a Lewis acid catalyst.

However, the intensity of the other weak bands at 1540 and 1557 cm^{-1} did not change with increase in temperature. This suggested presence of few isolated surface hydroxyls even at temperatures of 350 °C. However such hydroxyls are

Table 2
Activity-selectivity of the rutile catalyst R2 in relation to the anatase catalyst A2

Catalyst code	Chemicals for synthesis	Phase	Scherrer crystallite size (nm)	BET surface area (m^2/g)	Percentage conversion	Percentage ortho-selectivity
R2	$TiCl_3$, HNO_3, urea	Rutile	9.1	36	40	100
A2	$TiCl_3$, HNO_3 Urea, oxalic acid	Anatase	8.7	73	79	98

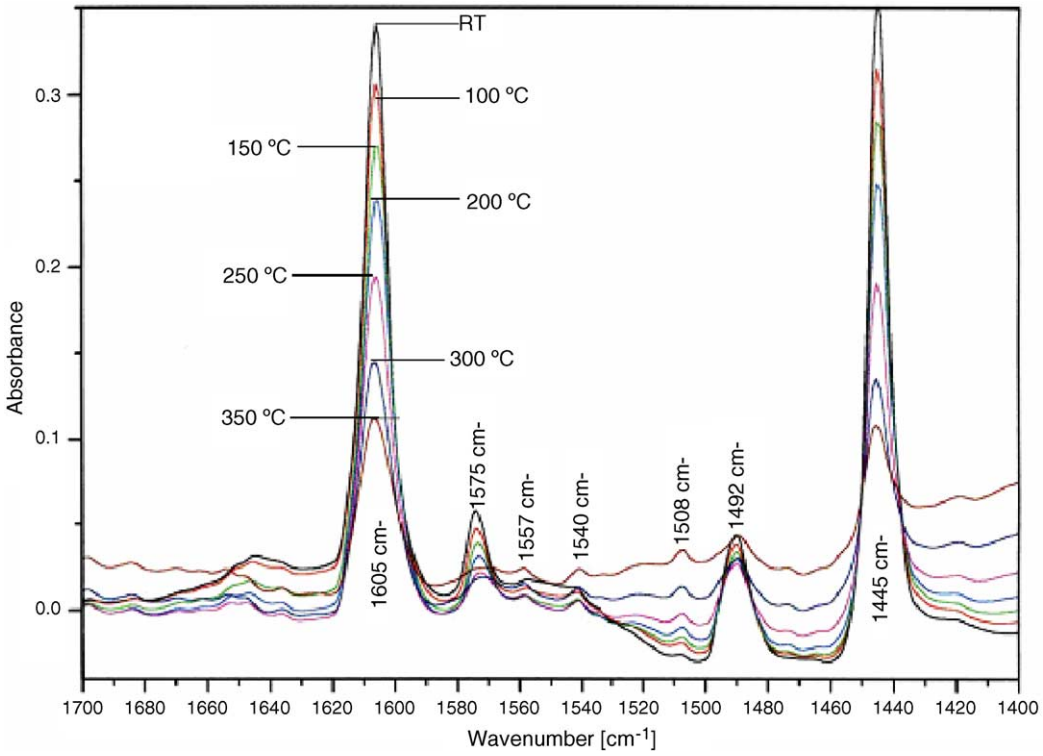

Fig. 3. In situ FTIR spectra of pyridine for R2 at different evacuation temperatures (ambient, 350 °C) in the frequency region 1400–1700 cm^{-1}. (The three weak bands at 1114, 1149 and 1217 cm^{-1} are not included in figure, but are shown in Table 2.)

reported to be lost at temperatures of about 400 °C [15,16] and, thus, would be absent under the reaction temperature employed during methylation of phenol.

Fig. 4 shows an overlay of the in situ FTIR spectra of R2 on A2. It is interesting to note that both the catalysts show similarity in band assignments although their intensities largely differ. The intensity of the Lewis acid site peaks in A2 is significantly less than the rutile catalyst R2. It could probably be due to lower concentration of acid sites in A2 in comparison to R2 as will be evident later from the TPD NH_3 spectra for acidity. In both the catalysts, the peaks at 1540, 1557 and 1574 cm^{-1} due to Bronsted acid sites are of much smaller intensities, while the peaks due to Lewis acidity at 1445 and 1605 cm^{-1} are the most intense. Since A2 has twice the catalytic activity as that of R2, it appears that the excess Lewis acid sites of R2 are of no consequence during catalytic methylation of phenol.

The concentration and strength of acidic as well as basic sites were further probed by temperature programmed desorption. Figs. 5 and 6 give the TPD spectra for desorption of CO_2 and NH_3, respectively on these catalysts. It is clear from the TPD CO_2 spectra in Fig. 5, that both these catalysts have

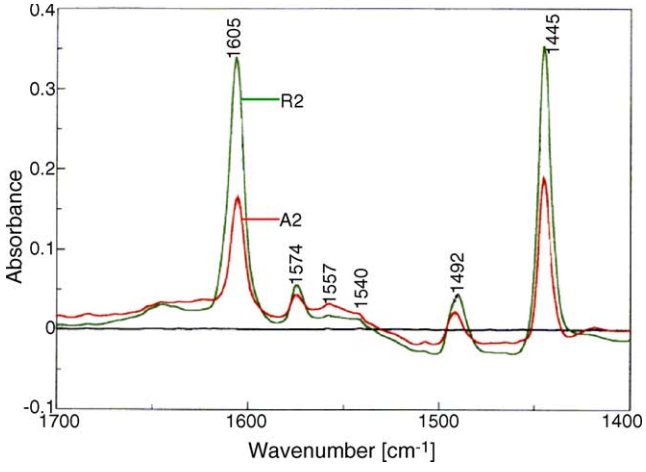

Fig. 4. In situ FTIR spectra of R2 and A2 after adsorption of pyridine, followed by evacuation at room temperature for 30 min.

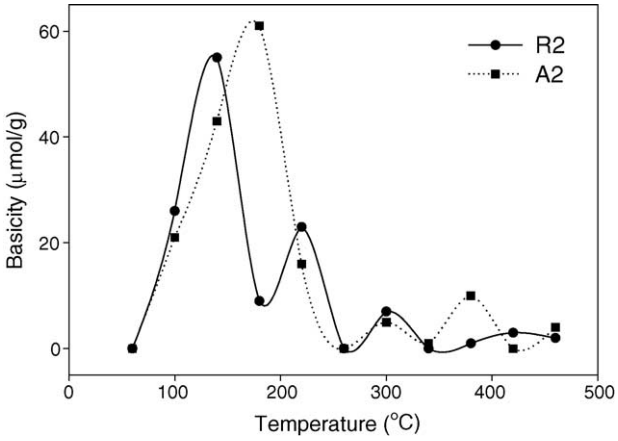

Fig. 5. TPD CO_2 spectra of TiO_2 catalyst: A2, pure anatase; R2, pure rutile.

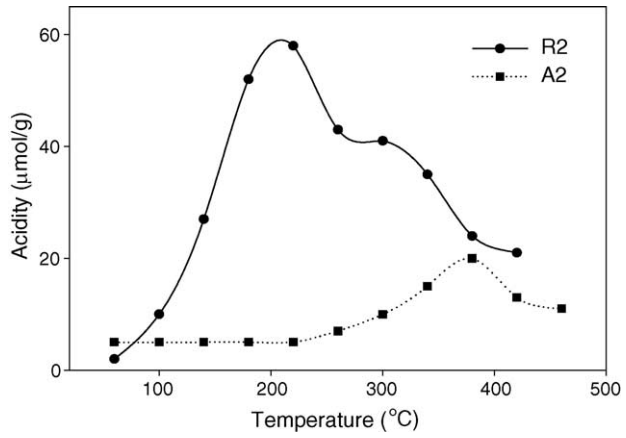

Fig. 6. TPD NH_3 spectra of TiO_2 catalyst: A2, pure anatase; R2, pure rutile.

similar distribution of basic sites. Both show a predominant peak due to weak basic sites, centered at ∼150 °C for R2 and ∼180 °C for A2. As reported earlier that these weak basic sites are essential for the high ortho-selectivity of R2. These weak basic sites assist in orienting the phenol molecule in a position perpendicular to the catalyst surface by causing electrostatic repulsions of the electron rich aromatic ring of phenol.

On the other hand, as seen from Fig. 6, R2 has large acidity, which is due to weak Lewis acid sites (peak ∼220 °C) and moderately strong Lewis acid sites (peak ∼320 °C). At the same time, A2 showed only one unique desorption peak at ∼380 °C mainly due to the presence of strong Lewis acid sites. Since A2 shows higher activity than R2, it seems that all the extra acidity in R2 is irrelevant for the observed activity-selectivity profiles in agreement with the above conclusion from in situ FTIR studies.

Thus based on the acid–base profile and the product distribution, it is proposed that the phenol molecule undergoes dissociative adsorption on a strong Lewis acid–weak Lewis base kind pair site.

3.2. Effect of oxalic acid on TiO_2 phase formation and catalytic activity

Since addition of oxalic acid in the synthesis procedure (A2) brought about a complete phase transformation from rutile to anatase, catalysts were prepared with varying quantities of oxalic acid so as to make mixed phase samples in order to study the effect of these mixed phases on active centers and corresponding methylation activity.

As mentioned in Section 2.1, these catalysts were synthesized using $TiCl_3$:oxalic acid:urea in the molar ratio of 1:*X*:2, where the moles of *X* was varied from 0 to 1 in steps of 0.2. For convenience sake, hereafter, these catalysts would be referred to as oxalic acid series.

The XRD spectra of these samples are already reported in Fig. 1. It is shown that by increasing the amount of oxalic acid, phase transition occurs from rutile to anatase. A 25 mol% of oxalic acid equivalent to 0.6 mol of oxalic acid in the present case was sufficient to bring about a complete phase transition. Their physical characteristics are given in Table 3.

It can be seen that the BET surface areas of the samples prepared using oxalic acid were generally large and increased as the oxalic acid content increased from 0 to 0.8. This is even when the scherrer crystallite sizes are almost the same in the range 8–11 nm, both for rutile, anatase as well as mixed phases. In fact, the pure rutile phase showed a relatively lower surface area ∼36 m^2/g as compared to the average surface area of 80 m^2/g for the other samples. The sample $RO_{0.2}$, which is rutile–anatase mixed phase in almost equal proportion, showed nearly twice the surface area as compared to the pure rutile phase. Thus, it is clear that the oxalic acid used in the synthesis is responsible for the enhancement in surface area of the TiO_2 catalysts. However, this enhancement in surface area appeared to reach a limiting value as the concentration of oxalic acid increased from 0.2 to 1 M.

3.3. Trends in activity-selectivity in the oxalic acid series

Fig. 7 shows the trends in activity of the series catalysts. For all the samples, the activity was found to increase with increase in temperature. It reached a maximum at 450 °C, beyond that the activity decreased.

Fig. 8 shows an interesting trend in catalytic activity in relation to the oxalic acid content of the samples. As the oxalic acid concentration increased from 0 to 0.6 the activity dropped and beyond that the activity steeply increased. Thus, the sample $RO_{0.6}$ showed the lowest activity of about 28%. Another interesting feature, as evident from Fig. 8, was that all the samples were highly ortho-selective, irrespective of the level of percentage conversion or activity. They showed >95% ortho-selectivity under all experimental conditions investigated. The catalyst $RO_{0.6}$ is a pure anatase sample while $RO_{0.2}$ and $RO_{0.4}$ showed increasing anatase phase. Thus, the high methylation activity of the TiO_2 catalysts is not merely phase (rutile or anatase) or surface area

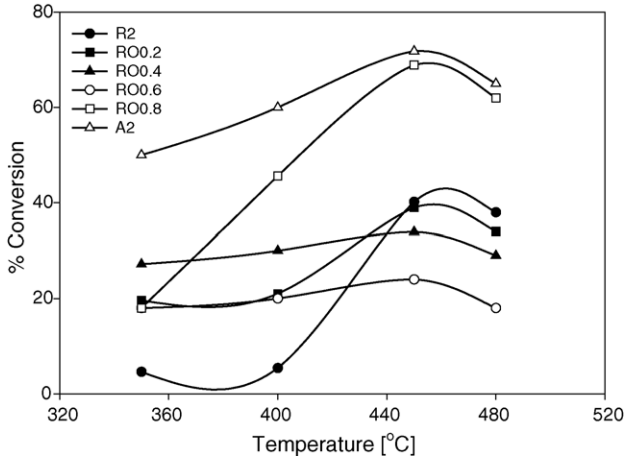

Fig. 7. Activity profiles of the TiO_2 catalysts synthesized as a function of the oxalic acid concentration.

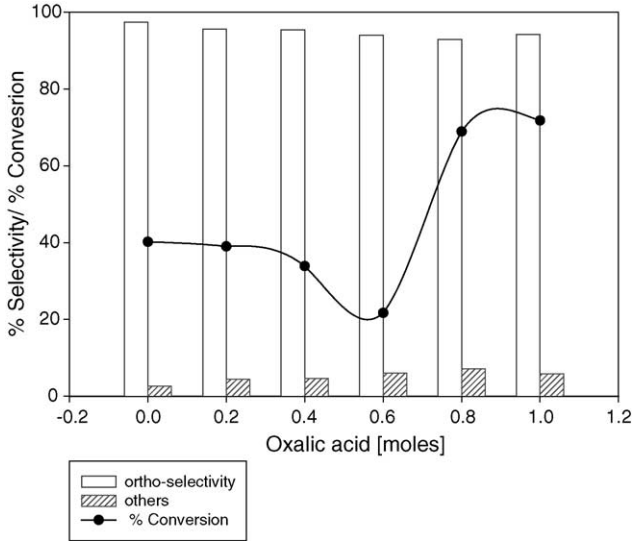

Fig. 8. The activity-selectivity profiles of the oxalic acid series catalysts as a function of oxalic acid content. Reaction conditions: 1 g of the catalyst; 1:6 phenol:methanol molar ratio; 5 ml/h flow rate and at a temperature of 450 °C.

dependent. The activity is, therefore, should be primarily dependent on the nature of active sites and porosity.

Figs. 9 and 10 show the TPD NH_3 and TPD CO_2 profiles, respectively, of all the TiO_2 samples in the series.

As can be seen from Fig. 10 all the samples showed a low temperature peak (<200 °C) in the TPD CO_2 spectrum corresponding to weak basic sites. Such weak basic sites are not reported on all TiO_2 samples or other oxides. There were slight shifts in the individual peak temperatures as well as differences in the intensities of the peaks. The total concentration of the weak basic sites (peak < 200 °C) is presented in Table 4. A quantitative approach is adopted for comparison of relative activity of the catalysts, as quantification of acid sites may not be accurate.

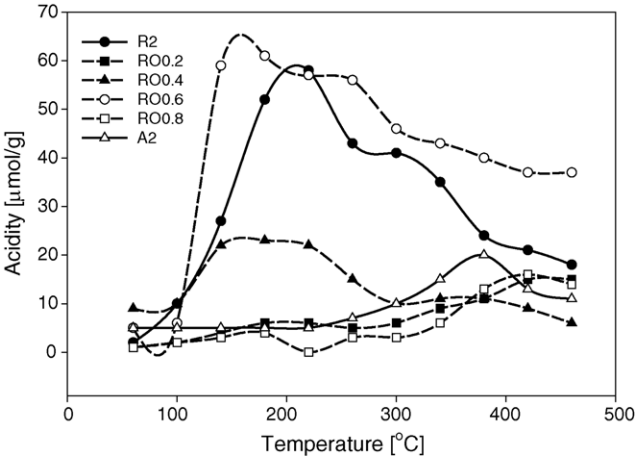

Fig. 9. TPD NH_3 spectra in TiO_2 catalysts synthesized as a function of the oxalic acid concentration. A2, pure anatase; R2, pure rutile; RO_x where $x = 0.2, 0.4, 0.6, 0.8$ denotes the concentration of oxalic acid in mol.

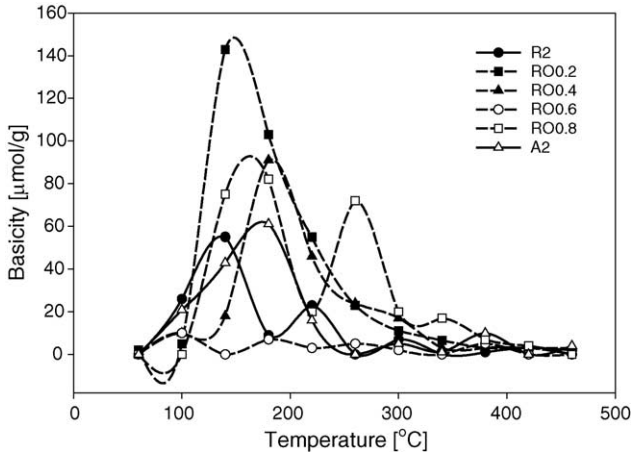

Fig. 10. TPD CO_2 spectra of the TiO_2 catalysts synthesized as a function of the oxalic acid concentration. A2, pure anatase; R2, pure rutile; RO_x where $x = 0.2, 0.4, 0.6, 0.8$ denotes the concentration of oxalic acid in mol.

Further, in the acidity profiles, Fig. 9 there was no distinct peak at around 380 °C for the various samples, which was identified in A2 as crucial for methylation activity. Most of the catalysts unlike A2, showed a very broad peak in the high temperature region ~350 °C. The concentration of these strong acid sites at 380 °C is similarly shown in the Table 4.

Following assumptions are made to determine the effective acid–base pairs responsible for catalytic activity/selectivity:

(i) It is primarily the strong Lewis acid–weak Lewis base (SA–WB) pairs that are responsible for the dissociative adsorption of phenol.
(ii) The weak base sites primarily help in perpendicular orientation of phenol. They are, hence, responsible for ortho-selectivity.
(iii) The lower numerical magnitude of either the strong Lewis acid site or weak Lewis base site would determine the effective concentration of SA–WB pairs. It is considered that one phenol molecule adsorbs per such SA–WB site.
(iv) The extra acidity or basicity of the catalyst did not seem to affect the methylation activity or selectivity significantly.

Accordingly the effective concentration of acid–base pairs is determined. It is shown in the last column in Table 4.

Fig. 11 shows the graph of effective site concentration and activity as a function of oxalic acid content overlaid on the corresponding catalytic activity profile. The nature of the two profiles indicates a close similarity in the trends, viz. the effective site concentration and the observed activity profiles. These results thus confirm that it is the SA–WB type of Lewis acid–base pairs that govern the methylation activity in these samples.

The discrepancy between the observed and calculated curves being due to the approximation in the quantification of the active sites and the difference in units for percentage

Table 4
Concentration of effective strong acid–weak base (SA–WB) pair sites in the oxalic acid series samples

Catalyst code	Strong acid (SA) sites (μmol/g)	Weak basic sites (μmol/g)	Effective SA–WB sites (μmol/g)
R2	24	100	24
$RO_{0.2}$	18	276	18
$RO_{0.4}$	15	218	15
$RO_{0.6}$	48	7	7
$RO_{0.8}$	21	28	21
A2	41	161	41

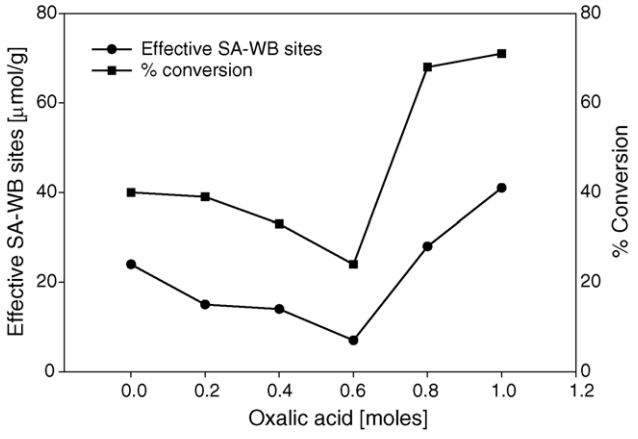

Fig. 11. Relation between the effective SA–WB (strong acid–weak base) Lewis sites and activity in TiO_2 catalysts synthesized as a function of the oxalic acid concentration.

conversion and concentration of sites. Nevertheless, the conclusions based on the above assumptions are inevitable.

3.3.1. Trends in individual selectivities towards o-cresol and 2,6-xylenol

It can be seen from Fig. 12 that as percentage conversion increases, the amount of 2,6-xylenol formed also increased. However, at the same time the selectivity towards *o*-cresol decreases. Thus, the sample $RO_{0.6}$, which shows minimum conversion of phenol, also shows minimum formation of 2,6-xylenol, but gives maximum formation of cresol. Similarly A2, which shows highest conversion as well as formation of 2,6-xylenol, gives minimum formation of *o*-cresol. Since these ortho products are of different molecular sizes, an attempt is made here to find correlation between the product selectivity and catalyst porosity.

The N_2 adsorption–desorption isotherms for two of the representative samples are as given in Fig. 13. A clear hysteresis at high relative pressure is observed, which is related to capillary condensation associated with large pore channels. The pore-size distribution as calculated from the desorption branch of the isotherm is represented in Fig. 14. Thus, TiO_2 samples synthesized in the present investigation were mesoporous in nature. However, they were not uniformly structured mesopores. It is clear that, addition of successively increasing amounts of oxalic acid during the synthesis affected the porosity of the samples, which, in turn, could control the product selectivity. Thus, as the oxalic acid content is increased, the intensity of the peak at 40 Å decreases while the distribution around the 80 Å peak increases. However, there is no clear peak at 80 Å across all the samples, instead a broad distribution of porosity is observed. Fig. 15 is a graph of the ratio of the intensities of the peak at 40 Å to that of the peak at 80 Å, in relation to the moles of oxalic acid used during the synthesis.

The correlation of the pore-size with selectivity is prominent in the anatase samples, i.e. with oxalic acid content more than 0.6. As can be seen from the figure that as the 40/80 ratio

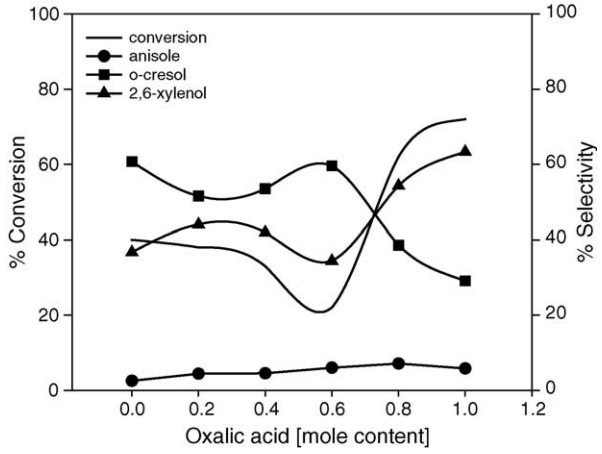

Fig. 12. Trend in formation of ortho-products, *o*-cresol and 2,6-xylenol in TiO_2 catalysts synthesized as a function of the oxalic acid concentration.

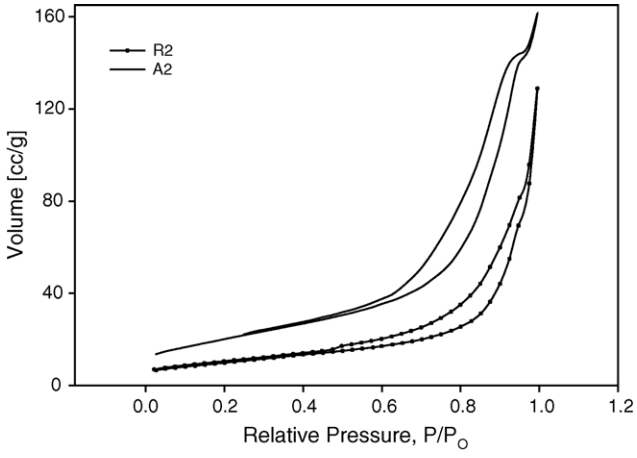

Fig. 13. BET N_2 adsorption–desorption isotherms for the catalysts R2 and A2.

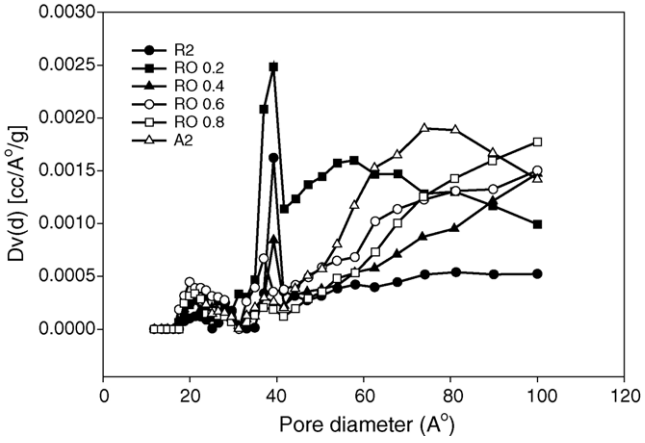

Fig. 14. Pore-size distribution of the TiO_2 catalysts synthesized as a function of the oxalic acid concentration.

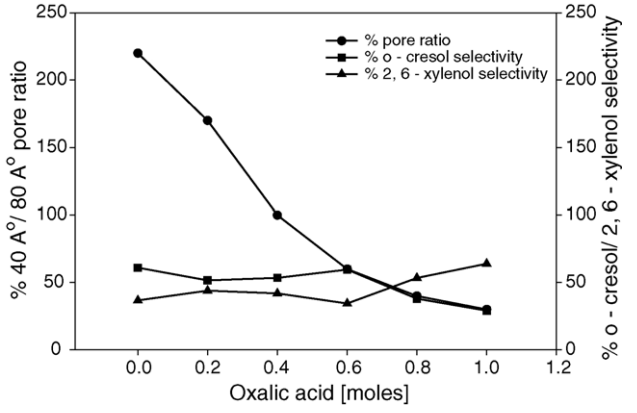

Fig. 15. Relation between the 40 and the 80 Å pore-size distribution and product selectivity in TiO_2 catalysts synthesized as a function of the oxalic acid concentration.

decreases the selectivity towards *o*-cresol also decreases. In other words, it is the 40 Å pores, which could be controlling the *o*-cresol formation. On the other hand, it appears that the pores of about 80 Å govern the formation of 2,6-xylenol.

4. Conclusions

1. TiO_2 is a versatile catalyst for methylation of phenol. Active rutile TiO_2 could be synthesized by $TiCl_3$–urea precursor, while active anatase could be obtained by additional use of oxalic acid. By varying the concentration of oxalic acid, it is possible to obtain pure and mixed phases of TiO_2, as desired.
2. Phase transition from rutile to anatase could be achieved with 25 mol% of oxalic acid.
3. Activity decreased upon phase transition to anatase with the minimum required oxalic acid of 25 mol%. The activity increased as anatase phase is synthesized with excess amount of oxalic acid.
4. Near 100% selectivity towards ortho products, viz. *o*-cresol and 2,6-xylenol.
5. Ortho-selectivity was found to be proportional to the effective strong Lewis acid–weak Lewis base pairs.
6. Internal variation between the *o*-cresol and 2,6-xylenol selectivity could be explained on the basis of catalyst pore-size. Thus, larger pore-size TiO_2 enhanced formation of 2,6-xylenol in preference to *o*-cresol.

Acknowledgements

The authors are grateful to Dr. Sajo P. Naik, University of Tokyo, Japan for his help in various ways. This research work was sponsored by UGC, New Delhi vide F-540/04/DRS/2003 (SAP-III).

References

[1] B. Viswanathan, Bull. Cat. Soc. India 10 (1–2) (2000) 1.
[2] A.R. Gandhe, J.B. Fernandes, Cat. Commun. 5 (2004) 89.
[3] A.R. Gandhe, J.B. Fernandes, J. Mol. Cat. 226 (2005) 171.
[4] S. Sato, K. Koizumi, F. Nozaki, J. Catal. 178 (1998) 264.
[5] R.A. Spurr, H. Myers, Anal. Chem. 29 (1957) 760.
[6] L. Bellami, Inostran. Liter. Moscow (1963) (in Russian).
[7] M. Herrmann, H. Boehm, Z. Anorg. Allg. Chem. B 358 (1967) 73.
[8] L. Little, Infrared Spectra of Adsorbed Molecules, Mir, Moscow, 1969 (in Russian).
[9] T. Bezrodna, G. Puchkovska, V. Shimanovska, I. Chashechnikova, T. Khalyavka, J. Baran, Appl. Surf. Sci. 214 (2003) 222.
[10] C. Bezouhanova, M.A. Al-Zihari, Appl. Catal. A 83 (1992) 45.
[11] T. Bezrodna, G. Puchkovska, V. Shimanovska, I. Chashechnikova, T. Khalyavka, J. Baran, Appl. Surf. Sci. 214 (2003) 222.
[12] E.P. Parry, J. Catal. 2 (1963) 371.
[13] D.K. Chakraborty, A. Ramachandran, in: N.M. Gupta, et al. (Eds.), Spectroscopic Methods in Heterogenous Catalysis, Tata McGraw Hill Publ. Co. Ltd., 1987, p. 36.
[14] V.D. Makwana, Y.-C. Son, A.R. Howell, S.L. Suib, J. Catal. 210 (2002) 46.
[15] M. Primet, P. Pichat, M. Mathieu, J. Phys. Chem. 75 (1971) 1216.
[16] M. Primet, P. Pichat, M. Mathieu, J. Phys. Chem. 75 (1971) 1222.
[17] M.R. Basila, J. Phys. Chem. 66 (1962) 2223.